ELSEVIER

Journal of Power Sources 80 (1999) 83–89

JOURNAL OF POWER SOURCES

# Dynamically compacted all-ceramic lithium-ion batteries

Michiel J.G. Jak [a,*], Frans G.B. Ooms [a], Erik M. Kelder [a], Waiter J. Legerstee [a], Joop Schoonman [a], Alfons Weisenburger [b]

[a] *Delft Interfaculty Research Center, Renewable Energy, Laboratory for Inorganic Chemistry, Delft University of Technology, Julianalaan 136, 2628 BL, Delft, Netherlands*

[b] *Forschungszentrum Karisruhe, Technik und Umwelt lnstitut fur Neutronenphysik und Reaktortechnik, P.O. Box 3640, D-76021, Karlsruhe, Germany*

Received 18 December 1998; accepted 23 December 1998

**Abstract**

This paper deals with a cell design and a unique manufacturing process for all solid-state lithium-ion batteries. Detailed analyses of the manufacturing of the components for such a battery and the compaction of the green battery are presented. The electrodes were made of coatings of $LiMn_2O_4$ on metal foils. The electrolyte was a free-standing foil of the ceramic electrolyte Li-doped $BPO_4$ in a polymer matrix. The different layers were wound and compacted by using magnetic pulse compaction. Several characteristics of the compacted batteries are presented. 

*Keywords:* Li-ion solid-state batteries; Electrolytes/solid inorganic; Manufacturing processes

## 1. Introduction

The large-scale introduction of Li-ion batteries for electric vehicles is hampered mainly by safety problems and cost aspects. The safety problems are related to leakage and decomposition of the liquid or polymer-based electrolyte, resulting in the formation of volatile and flammable gases [1–5]. The cost aspects are related to the expensive liquid or polymer-based electrolytes and the expensive production facilities, like dry-rooms, necessary when working with liquid or polymer-based electrolytes. Furthermore, Li-ion batteries using a liquid or polymer-based electrolyte have to be equipped with safety vents and adequate sealing is necessary [6].

The safety problems can be solved by using a thermally and electrochemically stable ceramic electrolyte with high ionic conductivity. A number of ceramic electrolytes with a high thermal and electrochemical stability and adequate ionic conductivity have been reported [7–15]. However, no significant cost reduction was established, due to high production costs caused by long synthesis times and high temperatures. Furthermore, the majority of these ceramics contain expensive metals, such as Ge, Ti, Sc, In, Lu, La, and Y.

Other disadvantages of using ceramic electrolytes are the inherently lower ionic conductivity compared with liquid and polymer electrolytes, as well as the poor interface contacts which usually exist between the ceramic electrolyte and the solid electrodes.

In this paper, a recently developed ceramic electrolyte and a production method that might contribute to a solution of all these problems will be presented. As an electrolyte, Li-doped $BPO_4$ seems to be a promising material for all-solid-state Li-ion batteries as it has an acceptable $Li^+$-ion conductivity and low production costs [16–21]. Magnetic pulse compaction (MPC) has been applied in order to improve the usually poor interfacial contacts between the ceramic electrodes and the ceramic electrolyte and also the densification of the layers themselves [22–25]. Component foils are laminated and pressed onto each other by using high-pressure pulses (i.e., dynamic compaction) resulting in improved interfaces.

The all-solid-state Li-ion battery manufactured with this proposed concept will be safe, cheap, and able to withstand high temperatures up to about 250°C. [21,26]. The production method and the battery characteristics will be discussed in detail.

* Corresponding author. Fax: +31-15-2788047; E-mail: m.jak@stm.tudelft.nl

0378-7753/99/$ - see front matter 
PII: S0378-7753(99)00064-6

## 2. Experimental aspects

### 2.1. Materials

The different battery components were made of foils consisting of powders of the active materials in a polymer matrix or with a polymer binder. The cathode material, $LiMn_2O_4$, (SEDEMA) was used as received. The $LiMn_2O_4$ was mixed with 10 wt.% carbon black (M.M.M.). The anode material was either synthetic graphite (Fluka) or $LiMn_2O_4$, (SEDEMA). Both anode materials were mixed with 10 wt.% carbon black (M.M.M.).

A total of 10 mol% Li-doped $BPO_4$ was used as the electrolyte material, which was made by a standard synthesis technique using $H_3BO_3$, $P_2O_5$, and $LiOH \cdot H_2O$ [16].

### 2.2. Foils

The anode and cathode materials were mixed with 10 wt.% PVDF (Solef, Solvay) and a solvent (1-methyl-2-pyrrolidone, $C_5H_9$ NO, Merck). The ratio of solid material to solvent was about 60:40 by weight. The cathode materials were coated on 15 μm aluminum foil by using a doctor blade. Similarly, the anode materials were coated on 20 μm copper foil. The layer thicknesses of both the anode, as well as the cathode, were in the range of 100 to 200 μm. Subsequently, the coatings were stored in a furnace at 150°C for at least 3 days prior to further processing.

The electrolyte was a free-standing foil (Solufill™, DSM Solutech) [27,28], in which the electrolyte powder was homogeneously dispersed in a polyethylene matrix. After extrusion of the mixture into a base-tape, biaxial stretching was applied in order to uniformly reduce the foil thickness down to the desired thickness. The foil thickness can be reduced down to 5 μm or even less with the proper starting powder. In this study, a foil thickness of about 60 μm was used. The density of the stretched foils can be increased by rolling or uniaxial pressing.

As an insulation foil, 50 μm Kapton™ (Dupont) was used. The insulation and electrolyte foils were cut into strips of 35 mm wide and about 300 mm long. The electrode foils were cut into strips of 30 mm wide and the same length. This difference in foil width was chosen to prevent short circuiting of the electrodes.

After drying of the foils, a green battery was made by winding the four separate foils on a copper core (diameter = 13 mm), as shown in Fig. 1. The cathode foil was taped onto the core to ensure electronic contact. The components of this green battery were wound until an external diameter of 16 mm was reached. The copper current collector of the anode foil was wrapped around the outside of the winding, ensuring electronic contact with the copper can. Subsequently, the foils were cut and the cell was taped. Finally, the green battery was placed into a copper tube with an internal diameter of 17 mm that fitted exactly around the green battery ensuring electronic contact of the copper current collector of the anode with the can.

### 2.3. Magnetic pulse compaction (MPC) [29–32]

The green battery, including the copper core and can, was compacted using MPC. With MPC, a high-energy pressure pulse can be generated with a typical pressure around 1 GPa and a pulse duration of about 200 μs. The MPC set-up consists of a bank of capacitors which is charged to a preset voltage between 1 and 3 kV, to give a maximum energy storage of 25 kJ. The charging voltage determines the delivered pressure. Via a spark gap, the stored energy is discharged through an induction coil (Fig. 2). By winding this coil in an appropriate way, a radial magnetic field that acts into the centre of the coil, is generated.

Any electronically conducting material in the coil will pick up this magnetic field and, as a result, will move in the direction of the centre. When the green battery is centred in the coil, the magnetic field will compress the copper can of the green battery, resulting in its compaction. After compaction of the battery, the powder particles within the components, as well as the separate battery components are pressed together.

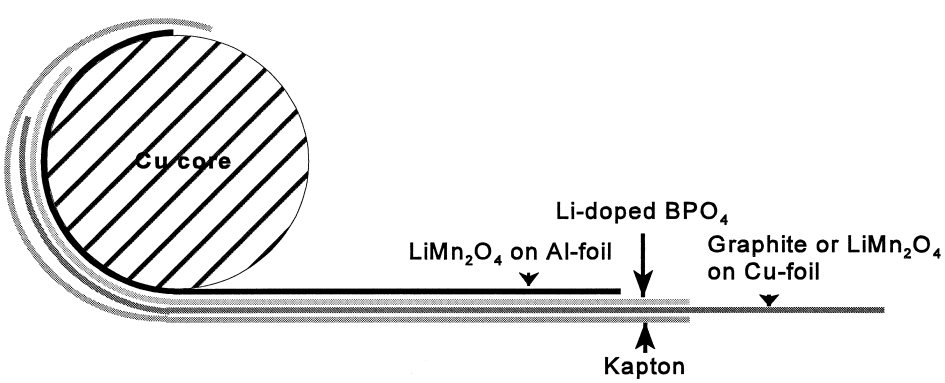


Fig. 1. Foil sequencing of the proposed battery configuration.

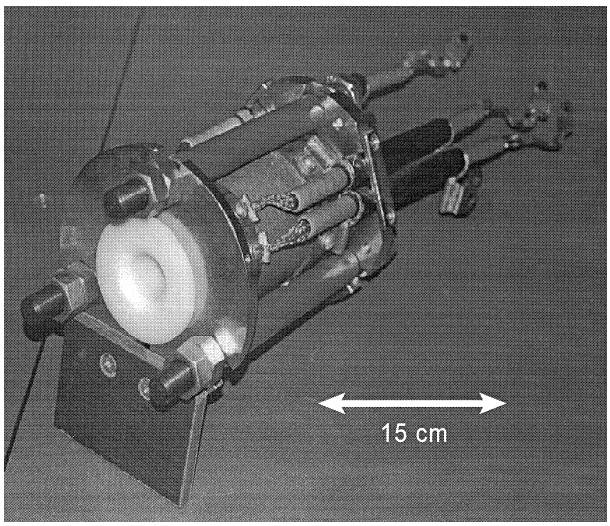


Fig. 2. Cylindrical coil magnetic pulse compactor (inner diameter = 20 mm).

### 2.4. Testing

The behaviour of the battery materials used, as a function of the applied high-pressures, has been studied in detail [16,22–24]. All the materials used show improved properties in terms of conductivity after dynamic compaction. The materials and foils for this series of experiments were studied by using Scanning Electron Microscopy (SEM, Jeol 5800 LV) and particle analysis (Fritsch Particle Size Analysette 22). The green and compacted batteries were tested using standard battery testing methods (Maccor Series 4000 battery tester).

## 3. Calculated performances

Based on the foil dimensions described in Section 2.2, the performance of the compacted batteries can be calculated. In this calculation, it was assumed that the internal resistance of the cell is determined only by the ionic conductivity of the composite solid electrolyte. Interfacial resistances and the electronic resistance of the electrodes were neglected. The total ionic conductivity of magnetic-pulse-compacted Li-doped $BPO_4$ is between $2 \cdot 10^{-6}$ and $5 \cdot 10^{-5}$ S $cm^{-1}$ at room temperature [16–19,21]. The ionic conductivity of magnetic-pulse-compacted Li-doped $BPO_4$ on Solufill™ foils is between $1 \cdot 10^{-7}$ and $5 \cdot 10^{-6}$ S $cm^{-1}$ [33]. In the following calculations, a conductivity of $2 \cdot 10^{-6}$ S $cm^{-1}$ will be used, hence, an electrolyte foil of 50 μm thickness and an area of 100 $cm^2$ results in an internal resistance of 25 Ω. The open circuit voltage of the cell is determined only by the electrodes. In case of a symmetrical configuration, i.e., $LiMn_2O_4$ used as anode as well as cathode, this results in an open circuit voltage of about 1 V. The capacity is determined by one of the electrodes, since the anode and the cathode are identical. A foil thickness of 100 μm and an area of 100 $cm^2$ will contain about 2 g of $LiMn_2O_4$ (50% dense). Assuming a practical specific capacity of 120 mA h $g^{-1}$ this will result in a capacity of 240 mA h.

The maximum useful current that can be delivered by the system can be calculated by assuming that the maximum internal resistance is 10% of the external resistance, resulting in a voltage drop of 0.1 V over the electrolyte. The current delivered by the system would then equal 0.1 V/25 Ω = 4 mA. The power of a cell with these characteristics would be 0.9 V × 4 mA = 3.6 mW.

Ionic conductivities of dynamically compacted Li-doped $BPO_4$ can be up to $2 \cdot 10^{-4}$ S $cm^{-1}$ [16], resulting in an internal resistance of 0.25 Ω, a current of 0.4 A, and a power of 0.36 W. A more detailed study of different configurations and related performances is given in Ref. [33].

## 4. Results and discussion

### 4.1. Foils

The agglomerate size of the dispersed powder particles determines the minimal foil thickness, i.e., the foils cannot be thinner than about five times the particle size of the dispersed powders. SEM and particle size analyses of $LiMn_2O_4$ and Li-doped $BPO_4$, show particle sizes of 25 and 10 μm, respectively. The particle size of carbon black is much smaller then that of the $LiMn_2O_4$ and is, therefore, not relevant with regard to foil thickness.

In Fig. 3, a cross-section of the Solufill™ electrolyte foil is shown. After biaxial stretching, a layered matrix of polyethylene with homogeneously dispersed Li-doped $BPO_4$ particles is visible. The cross-section of the electrode foil shows a completely different morphology (Fig. 4). In this case, the polymer serves as a binder between the powder particles (Fig. 5) instead of a polymer matrix as

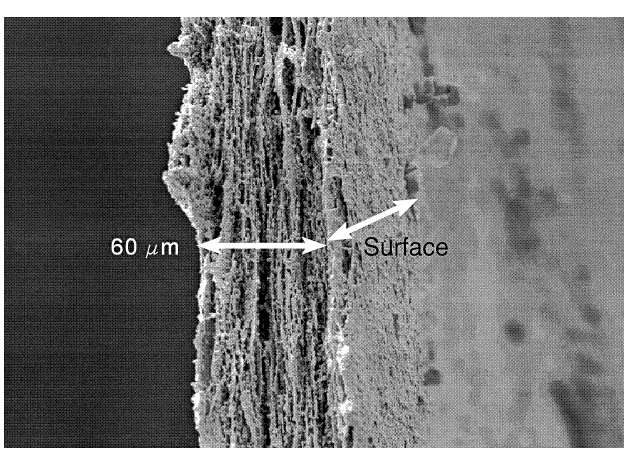


Fig. 3. Cross-section of Li-doped $BPO_4$ electrolyte coating on Solufill™ foil.

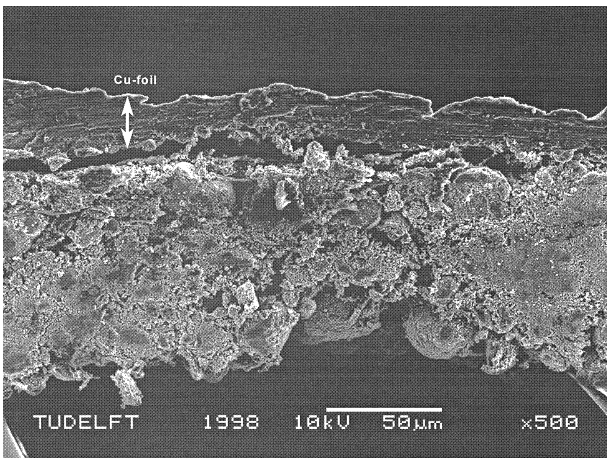


Fig. 4. Cross-section of $LiMn_2O_4$ + carbon black + PVDF coating on copper foil.

obtained with the electrolyte foil. The polymer content of both foils is comparable.

### 4.2. Winding and compaction results

The first green battery was wound on a 4 mm diameter copper core with foil lengths of approximately 100 cm. The foils were wound by hand using a simple homemade foil winder, without applying any tension to the foils or pressure on the core. As a result, the green density was very low. In the case of compaction of a green battery with loose windings, as shown in Fig. 6, the low starting density leads to a relatively large decrease in diameter, resulting in a compact which has the same shape as the applied magnetic field. In this case, the compacted cell will have an internal resistance that varies throughout the winding, leading to different current densities, and resulting in hot spots which may be detrimental to the cell.

Furthermore, the geometry of the cross-section in the middle of the cell is no longer spiral but a starlike pattern


Fig. 5. Surface of $LiMn_2O_4$ + carbon black + PVDF coating on copper foil.

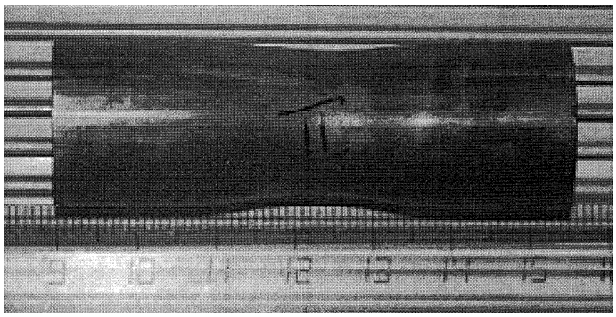

Fig. 6. Magnetically pulse-compacted battery (loosely wound foils, each 100 cm long, 4 mm diameter copper core).

is observed instead (Fig. 7). Due to these deformations, short-circuiting and current density variations may occur. The reason for this deformation is caused by the large decrease in diameter. The spirally wound cell is forced to decrease only in diameter, resulting in wrinkling of the foils whose lengths stay the same. To solve the problem of this large decrease in diameter, two options are possible:

(a) using a thicker core, so leading to fewer windings and, therefore, a smaller decrease in diameter
(b) tighter winding of the foils.

Of course, option (a) will reduce the specific capacity of the cell. A decrease of the applied pressure will result in a poor interface contact and is, therefore, no option.

An example of a compacted cell with a thicker core is shown in Fig. 8. A very homogeneous and non-deformed compact is obtained.

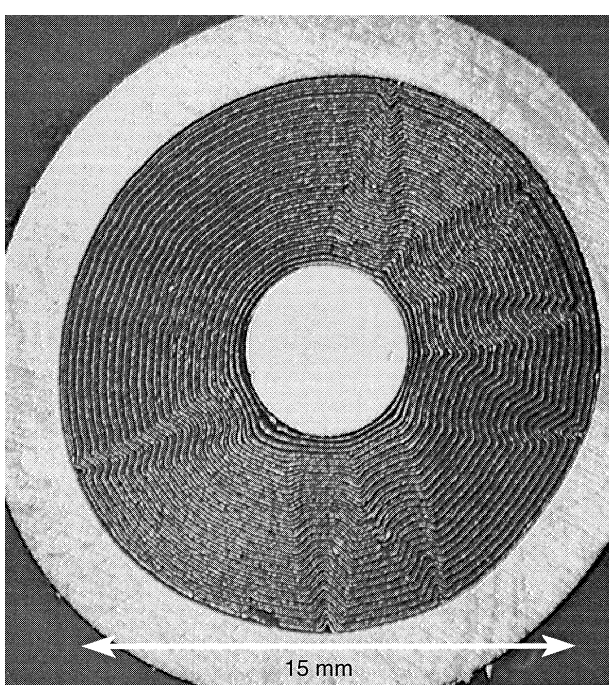


Fig. 7. Cross-section of magnetically pulse-compacted battery shown in Fig. 6, with loosely wound foils.

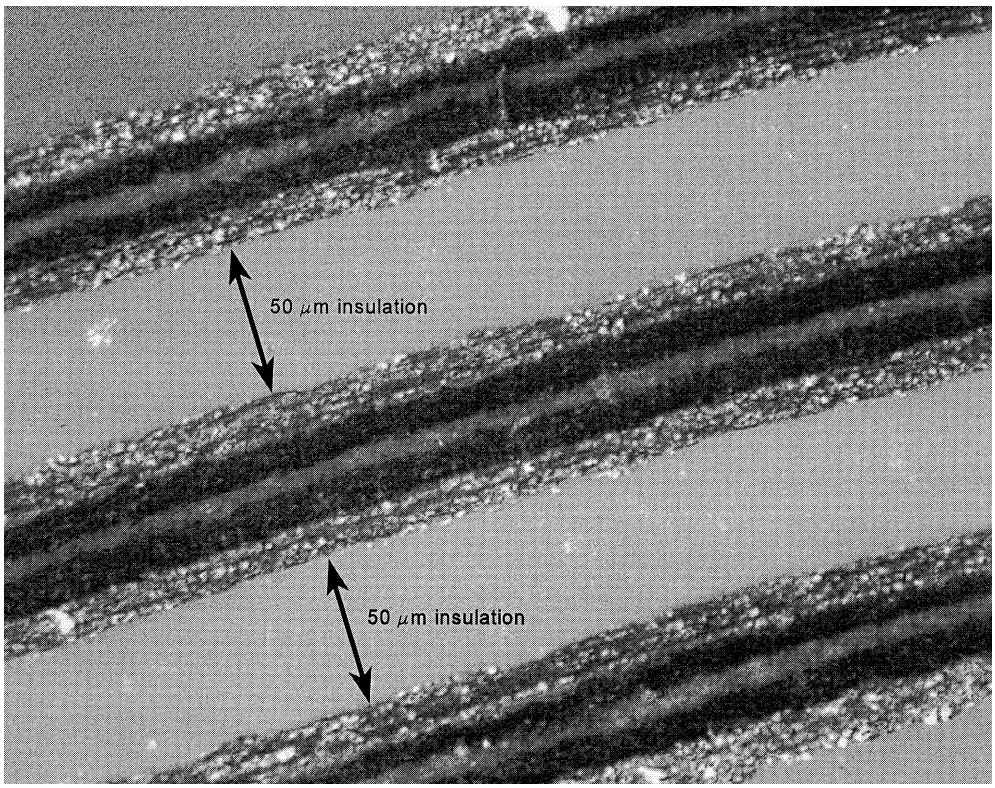


Fig. 8. Detail of cross-section of a magnetically pulse-compacted battery with a thick, 13 mm, copper core. White layer: insulation (Teflon, 50 μm), shiny layers: current collectors (Al foil, 10 μm), black layers: electrodes ($LiMn_2O_4$ on foil, 10 μm), grey layer: electrolyte (Li-doped $BPO_4$ electrolyte coating on Solufill™ foil, 10 μm).

An example of 'proper' winding is shown in Fig. 9. In this case, the foils were wound with a commercial winder (Montena) with tension applied to the foils and rollers pressing these foils onto those already wound onto the core. As a result, a much higher green density is obtained, leading to a smaller decrease in diameter on compaction.

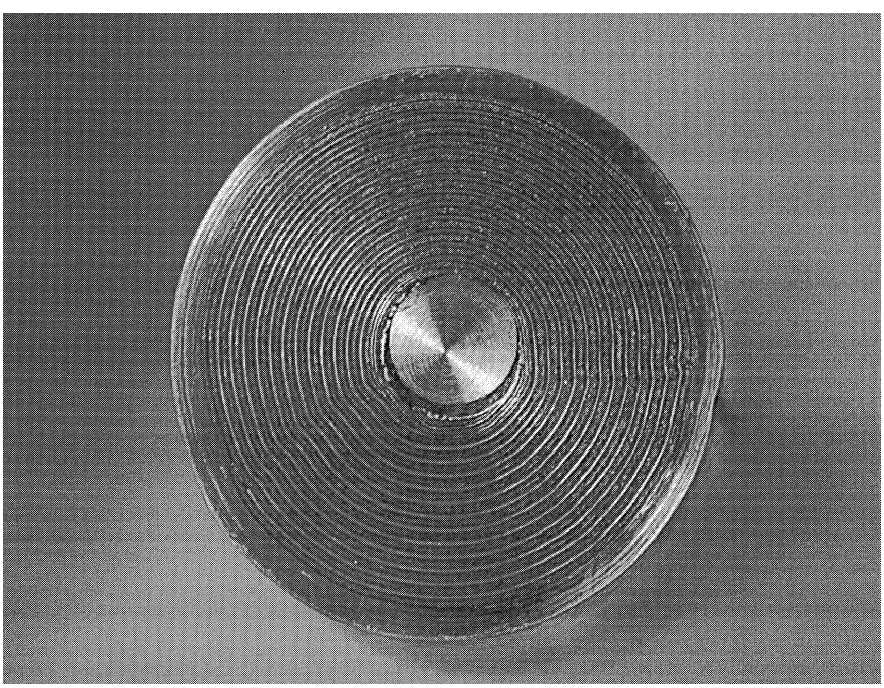

Fig. 9. Cross-section of a magnetically pulse-compacted battery (tightly wound foils).

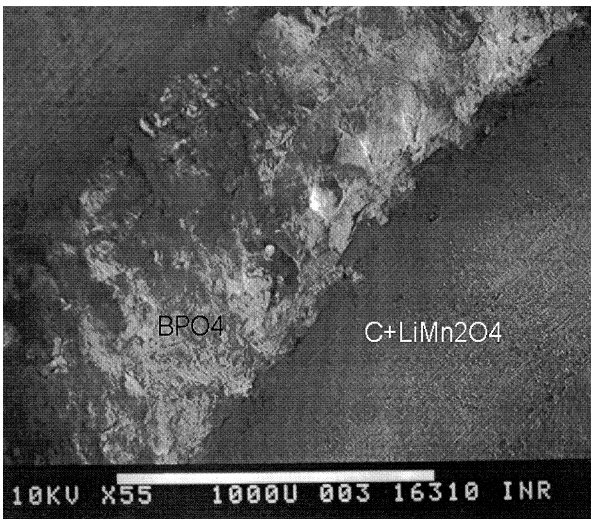


Fig. 10. Cross-section of magnetically pulse-compacted flat cell.

The examples described point out the importance of proper winding. As shown in Fig. 9, the geometry of the compacted cell is identical to that of the green battery, without any wrinkling that could lead to short-circuiting and current density deviations.

A more detailed SEM analysis of the cross-sections shows the intimate contact between the different components. For this analysis, a cell consisting of thicker foils with the same composition, was compacted uniaxially with a comparable pressure. The only relevant difference in this experiment was the large particle size of the electrolyte, which was in the range from 50 to 100 μm. A cross-section of the cell is shown in Fig. 10. A representative detail of the electrolyte/electrode interface is depicted in Fig. 11, showing very intimate contact between the different layers, proving the applicability of the dynamic compaction technique.

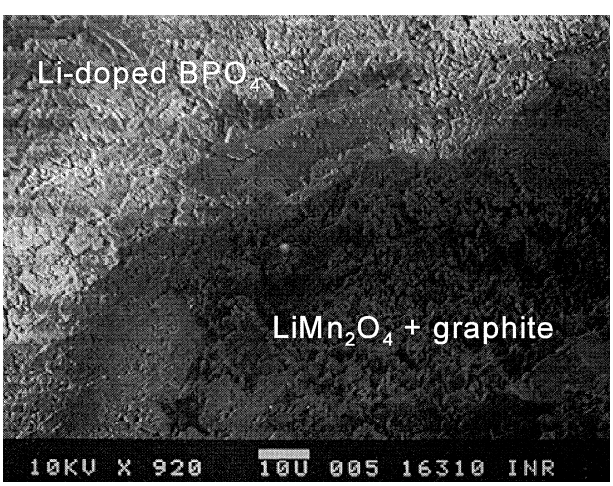


Fig. 11. Detail of cross-sectional interface between $LiMn_2O_4$ and Li-doped $BPO_4$ for the battery of Fig. 10.

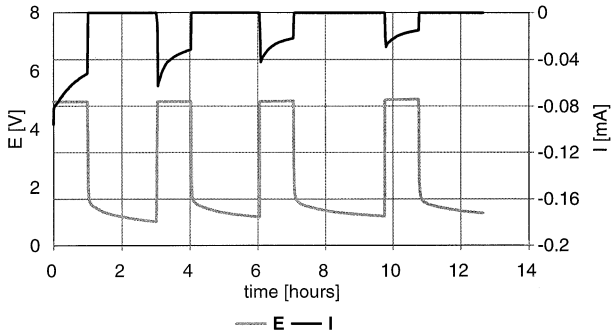


Fig. 12. Current and voltage against time during 5 V pulsed charging.

### *4.3. Battery characteristics.*

Prior to compaction, the internal resistance of the green battery with a foil area of 40 $cm^2$ was 200 kΩ. After compaction, the internal resistance of the uncharged battery was 150 Ω and after charging 8.3 kΩ. This increase in internal resistance must be caused by either the interfaces between the electrolyte and electrodes and/or the electrodes themselves, since the conductivity of the electrolyte is constant. The small changes in lattice parameters of $LiMn_2O_4$ during cycling will be compensated by the polymer binder, and therefore, will not lead to a delamination of the cell. The increase in internal resistance could be caused by changes in the conductivity of the $LiMn_2O_4$.

The calculations for an unchanged, 100 $cm^2$, compacted battery resulted in an internal resistance of 25 Ω, which is equal to 62.5 Ω after correction for the smaller area. The reason for the higher measured internal resistance could be the contribution of the electrodes, interfacial resistances, porosities, and/or the influence of the polymer binder in the electrolyte foil.

The batteries, as compacted, were tested with a Maccor battery tester and some characteristics are highlighted here. The symmetrical cells have an open circuit voltage between 1.0 and 1.2 V. The current and voltage graphs during charging at 5 V and open-circuit relaxation are plotted in Fig. 12. These results confirm the stability of the system up to at least 5 V. The high internal resistance is due to the fact that, prior to this charging, the battery's internal resistance had been measured and therefore, the battery was already charged to some extent.

A more extensive study of the battery characteristics will be published in a forthcoming paper.

## 5. Conclusions

MPC proved to be a suitable technique for the compaction of all-solid-state Li-ion batteries. Intimate interface contacts between the different cell components and densifi-

cation of the individual components were obtained. Charging these batteries at 5 V was shown to be possible.

The detrimental consequence of poor winding emphasized the importance of proper winding, which resulted in homogeneous compacts and a preserved geometry after compaction.

Optimization of foil processing and improvement of the ceramic electrolyte are the most important issues for the realization of practical batteries.

## Acknowledgements

The authors would like to thank Ing. N. van Landschoot and Mr. S.J. Everstein for their assistance with synthesis and analysis of the materials. Montena America (USA), SEDEMA (Belgium), and IAP Research (USA) are acknowledged for the winding experiments, $LiMn_2O_4$ samples, and MPC, respectively. The European Science Foundation is acknowledged for support for travelling via the ESF-NANO programme. DSM Solutech (The Netherlands), Shell IEP (The Netherlands), and the Foundation for Chemical Research in The Netherlands (NWO-CW), and the Technology Foundation (STW) under the Netherlands Organization for Scientific Research (NWO) are gratefully acknowledged for their financial support.

## References

[1] P. Arora, R.E. White, M. Doyle, J. Electrochem. Soc. 145 (1998) 3647.
[2] L.A. Dominey, in: G. Pistoia (Ed.), Lithium Batteries, Industrial Chemistry Library, Vol. 5, Elsevier, Amsterdam, 1994, p. 278.
[3] Z.X. Shu, R.S. McMillan, J.J. Murray, J. Electrochem. Soc. 140 (1993) Ll01.
[4] Z. Jiang, M. Alamgir, K.M. Abraham, J. Electrochem. Soc. 142 (1995) 333.
[5] H. Moa, J.N. Reimers, Q. Zhong, U. von Sacken, Electrochem. Soc. Proc. 9–28 (1995) 245.
[6] S. Hossain, in: D. Linden (Ed.), Handbook of Batteries, Chap. 36, 2nd edn., McGraw-Hill, New York, 1995.
[7] R.D. Shannon, B.E. Taylor, A.D. English, T. Berzins, Electrochem. Acta 22 (1977) 783.
[8] E.I. Burmakin, I.G. Sheckman, G.K. Stepanov, Sov. Electrochem. 18 (1982) 248.
[9] C.K. Lee, A.R. West, J. Mater. Chem. 1 (1991) 149.
[10] R.A. Huggins, Electrochem. Acta 22 (1977) 773.
[11] J.J. Carillo-Lazo, P. Quintana, A. Huanosta, Solid State Ionics 73 (1994) 169.
[12] A. Khorassani, A.R. West, J. Solid State Chem. 53 (1984) 369.
[13] H. Aono, E. Sugimoto, N. Imanaka, G. Adachi, J. Electrochem. Soc. 137 (1990) 1023.
[14] J.B. Bates, N.J. Dudney, G.R. Gruzaiski, R.A. Zuhr, A. Choudhury, C.F. Luck, J.D. Robertson, Solid State Ionics 53–56 (1992) 647.
[15] X. Yu, J.B. Bates, G.E. Jellison Jr., F.X. Hart, J. Electrochem. Soc. 144 (1997) 524.
[16] M.J.G. Jak, E.M. Kelder, N.M. van der Pers, A. Weisenburger, J. Schoonman, J. Electroceramics 2 (1998) 127.
[17] E.M. Kelder, M.J.G. Jak, F. de Lange, J. Schoonman, Solid State Ionics 85 (1996) 285.
[18] M.J.G. Jak, E.M. Kelder, J. Schoonman, J. Solid State Chem., 1998, in press.
[19] M.J.G. Jak. E.M. Kelder, Z.A. Kaszkur, J. Pielaszek, J. Schoonman, Solid State Ionics, 1998, in press.
[20] M.J.G. Jak, V.W.J. Verhoeven, I.M. de Schepper, F.M. Mulder, E.M. Kelder, J. Schoonman, Physica B, 1998, submitted.
[21] M.J.G. Jak, E.M. Kelder, S.J. Everstein, J. Schoonman, J. Power Sources, 1998, submitted.
[22] M.J.G. Jak, E.M. Kelder, M. Stuivinga, J. Schoonman, Solid State Ionics 86–88 (1996) 897.
[23] M.J.G. Jak, E.M. Kelder, A.A. van Zomeren, J. Schoonman, 8th Int. Meeting on Lithium Batteries, Extended Abstracts, June 1996, Nagoya, Japan, 1996, p. 322.
[24] M.J.G. Jak, E.M. Kelder, A.A. van Zomeren, J. Schoonman, in: W.A. Adams, B. Scrosati, A.R. Landgrebe (Eds.), Exploratory Research and Development of Batteries for Electric and Hybrid Vehicles, PV96-14, The Electrochemical Society Proceedings Series, Pennington, NJ, 1996, p. 58.
[25] M.J.G. Jak, E.M. Kelder, J. Schoonman, Patent PCT/NL96/00356, September 11, 1996.
[26] M.J.G. Jak, E.M. Kelder, Z.A. Kaszkur, J. Pielaszek, V.W.J. Verhoeven, J. Schoonman, The Electrochemical Society Proceedings Series, Pennington, NJ, 1998, submitted.
[27] J. Schoonman, E.M. Kelder, V.E.J. van Dieten, Extended Abstracts, 95-2, The Electrochemical Society, Abstract No. 580, Chicago, IL, October 8–13, 1995, p. 929.
[28] J. Schoonman, E.M. Kelder, J. Power Sources 68 (1997) 65.
[29] T. Negishi, T. Ogura, T. Masumoto, T. Goto, K. Fukuoka, Y. Syono, H. Ishii, J. Mater. Sci. 20 (1985) 399.
[30] V. Ivanov, S. Paranin, A. Vikhrev, R. Bbhme, G. Schumacher, Proc. 4th Euro Ceramics, 2, Riccione, 1995, p. 169.
[31] V. Ivanov, Y.A. Kotov, O.H. Samatov, R. Bbhme, H.U. Karow, G. Schumacher, Proc. International Conference Nanostructured Materials, Stuttgart, 1994.
[32] R. Bbhme, M.J.G. Jak, G. Link, A. Weisenburger, Abstract of the ESF-NSF symposium: Aerosols for Nanostructured Materials and Devices, Edinburgh, 1998, p. 42.
[33] E.M. Kelder, M.J.G. Jak, J. Schoonman, The Electrochemical Society Proceedings Series, Pennington, NJ, 1998, submitted.